

# LAMBERT: Layout-Aware language Modeling using BERT for information extraction\*

**Łukasz Garncarek** and **Rafał Powalski** and **Tomasz Stanisławek** and **Bartosz Topolski**<sup>†</sup>  
Applica.ai, Zajęcza 15, 00-351 Warszawa (Poland)  
firstname.lastname@applica.ai

**Piotr Halama**  
Applica.ai, Zajęcza 15  
00-351 Warszawa (Poland)  
piotr.halama@applica.ai

**Filip Graliński**  
Applica.ai, Zajęcza 15  
00-351 Warszawa (Poland)  
Adam Mickiewicz University  
Wieniawskiego 1, 61-712 Poznań (Poland)  
filip.gralinski@applica.ai

## Abstract

In this paper we introduce a novel approach to the problem of understanding documents where the local semantics is influenced by non-trivial layout. Namely, we modify the Transformer architecture in a way that allows it to use the graphical features defined by the layout, without the need to re-learn the language semantics from scratch, thanks to starting the training process from a model pretrained on classical language modeling tasks.

## 1 Introduction

The inherent sequential structure of natural language leads to the usual practice of treating text as a sequence of tokens, characters, or—more recently—subword units. In many Natural Language Processing (NLP) related problems, this linear perspective is sufficient and has led to significant breakthroughs, such as the introduction of Transformer neural architecture (Vaswani et al., 2017). This linear perspective currently remains as the basis of the state-of-the-art models in NLP problems. Interestingly, contrary to recurrent neural networks, the sequential nature of language is not reflected directly in the network architecture.

In this setting, the task of computing token embeddings is solved by Transformer encoders, such as BERT (Devlin et al., 2019) and its modifications such as RoBERTa (Liu et al., 2019b), or ALBERT (Lan et al., 2019). These encoders achieved

top scores on the GLUE benchmark (Wang et al., 2019). Other, non-BERT-derived architectures include Transformer-XL (Dai et al., 2019), XLNet (Yang et al., 2019), GPT (Radford, 2018), and GPT-2 (Radford et al., 2019).

They all deal with problems arising in texts defined as sequences of words. However, in many cases a structure more intricate than just a linear ordering of tokens is available. This is the case for printed or richly formatted documents, where different styles of headers, relative vertical and horizontal positions of tokens contained in tables, or spacing between paragraphs, all carry useful information. After all, the very goal of endowing texts with non-trivial layout and formatting is to improve readability.

There are two main lines of research on understanding documents with non-trivial layout. The first one is Document Layout Analysis (DLA), the goal of which is to identify contiguous blocks of text and other non-textual objects on the page and determine their logical function and order in the document.

Many services utilize DLA functionality for OCR (which requires document segmentation), table detection, or form field detection, and their capabilities are still being expanded. The most notable examples are Amazon Textract (Amazon, 2019), Google Cloud Document Understanding AI platform (Google, 2019), and Microsoft Cognitive Services (Microsoft, 2019). However, they have their limitations, such as the need to create rules for extracting information from the tables recognized by the system.

After the layout of the document has been ana-

\* Work in progress; this version of the paper was submitted to ACL2020 on December 10, 2019, and withdrawn on February 17, 2020

<sup>†</sup> The authors ŁG, RP, TS, and BT have equally contributed to the paper and are listed in alphabetic order

lyzed, the obtained segmentation can be combined with the textual information contained in the detected blocks. Such a method has been employed by Liu et al. (2019a).

The second approach is to directly combine the methods of Computer Vision and Natural Language Processing, for instance by representing a text-filled page as a multichannel image, with channels corresponding to the features encoding the semantics of the underlying text, and then using convolutional networks. This method was used, among others, by Katti et al. (2018); Denk and Reisswig (2019).

We decided to take yet another approach, similar to the one recently also used by Rahman et al. (2019), which is to inject the layout information into a modified variant of an already pretrained BERT instance, and fine-tune the extended model on datasets containing additional layout features. What makes our work completely different is that while Rahman et al. (2019) consider texts accompanied by audio-visual signal, we apply the idea of extending input embeddings to additional features extracted from formatted texts.

Building on a pretrained model has an important advantage; producing a dataset containing text with positional information and non-trivial layout is more difficult than creating a dataset for standard language modeling. The datasets we use are orders of magnitude smaller than the ones used to train BERT and are not large enough to train from scratch. By using pretrained models, we preserve the representations already learned from significantly larger training corpora.

## 2 Problem description

### 2.1 Data model

The data we are working with is usually produced by OCR systems, and so we will accommodate the characteristics of OCR output into our data model. Such output usually has the form of a sequence of tokens, together with their bounding boxes in the form  $(x_1, y_1, x_2, y_2) \in \mathbb{R}^4$  and additional segmentation information—tokens can be grouped into segments (e.g. lines, paragraphs, table cells, whole pages), each having its own bounding box.

In our data model, a document consists of the following data:

1. a list of tokens ( $t_i$ ),
2. a list of token bounding boxes ( $b_i$ ),

3. a collection of *segmentations*, where a segmentation is a partition of the set of all tokens into *segments*, together with a bounding box for each segment.

We will consider only single-page documents, which means that longer documents are divided into separately processed pages. It is also assumed that there is always a trivial segmentation corresponding to the whole page, containing all the tokens, so that we are always given the bounding box of the page. We can also think of tokens as 1-element segments, making segments the basic object in all layout considerations.

It is assumed that the tokens are given in the form of an ordered list. This is the case for OCR systems, and also other tools such as PDFMiner (Shinyama, 2019), which we used to process PDF documents. Although the produced order does not always perfectly correspond to the reading order, it is close enough. We might be tempted to deliberately discard this sequential information and force the model to learn it from the joint semantic and positional representations. However, in our approach, this strategy is impossible because our solution relies on modifying already pretrained models, which require the sequential information. Nonetheless, we manage to gradually reduce the importance of the sequential order during training (see Section 4.3)

Finally, note that such a data model preserves not only the relative positions of tokens on the page, significant in case of tables, but also some style information, encoded in the relative heights of bounding boxes, which may be helpful for determining important contextual information such as section titles.

### 2.2 Problem statement

Suppose we are given a document in the form of a sequence of tokens and their bounding boxes as described in Section 2.1, together with the bounding box of the page, and possibly additional segmentation produced by the OCR system. Our aim is to construct a sequence of corresponding contextualized embeddings  $v_i$ , where  $v_i \in \mathbb{R}^d$  for some fixed dimension  $d$ , taking into consideration not only the semantics of the text, but also the positional information encoded in the sequence of bounding boxes of tokens and/or segments.

### 3 Proposed method

#### 3.1 Background

The basic Transformer encoder, used in, for instance, BERT, is a sequence-to-sequence model transforming a sequence  $x_i \in \mathbb{R}^n$  of input embeddings into a sequence of output embeddings  $y_i \in \mathbb{R}^m$  of the same length, for the input/output dimensions  $n$  and  $m$ . One of the main distinctive features of this architecture is that it discards the order of its input vectors, enabling parallelization impossible for traditional recurrent neural networks.

In such a setting, the information about the order of tokens is preserved not by the structure of the input, but instead passed explicitly to the model, by defining the input embeddings as

$$x_i = s_i + p_i, \quad (1)$$

where  $s_i \in \mathbb{R}^n$  is the semantic embedding of the token at position  $i$ , taken from a trainable embedding layer, while  $p_i \in \mathbb{R}^n$  is a positional embedding, depending only on  $i$ .

Since in BERT the embeddings  $p_i$  are trainable, the number of pretrained embeddings defines a limit on the length of input sequence, in our case 512.

#### 3.2 Proposed solution

In order to inject layout information into a pretrained BERT model we modify the input embeddings defined in eq. (1), by adding a new term. Namely, using the notation from Section 3.1, we define

$$x_i = s_i + p_i + \ell_i, \quad (2)$$

where  $\ell_i \in \mathbb{R}^n$  depends on a *context embedding*  $c_i \in \mathbb{R}^k$ , encoding the layout information carried by the token’s location on the page (context embeddings will be explained in more detail in the next section). More precisely, we put

$$\ell_i = L(c_i), \quad (3)$$

where  $L : \mathbb{R}^k \rightarrow \mathbb{R}^n$  is a trainable linear layer, whose weight matrix is initialized according to a normal distribution  $\mathcal{N}(0, \sigma^2)$ , with the standard deviation  $\sigma$  being a hyperparameter.

The use of the linear layer  $L$  enables the pretrained model to gradually learn how to use additional information coming from the context embeddings. That is why we have to choose  $\sigma$  carefully, so that in the initial phase of training, the  $\ell_i$  term

does not interfere with the already learned representations. We experimentally determined the value  $\sigma = 0.02$  to be near-optimal.

#### 3.3 Context embeddings

Recall that in our setting, a document is represented by a sequence of tokens (or, more generally, segments)  $t_i$  and their bounding boxes  $b_i$ . To each element of this sequence, we assign its context embedding  $c_i$ , carrying the information about the position of the token with respect to the whole document. This can be done in various ways. What they all have in common is that the embeddings  $c_i$  depend only on the bounding boxes  $b_i$  and not on the tokens  $t_i$ .

As mentioned, this also is the moment where segmentations come into play. Since the context embeddings are supposed to depend only on bounding boxes, they can be computed for any segmentation, and the token embeddings can be taken to be the embeddings of the segments they are contained in.

In this paper, we compare three alternative context embeddings, described in the following subsections.

##### 3.3.1 Winding embeddings

For  $j = 1, \dots, d$  and scaling factors  $\theta_r \in \mathbb{R}$ , define a function  $F^\theta : \mathbb{R} \rightarrow \mathbb{R}^d$  by

$$F_j^\theta(t) = \begin{cases} \cos(\theta_r t) & \text{if } j = 2r \\ \sin(\theta_r t) & \text{if } j = 2r + 1. \end{cases} \quad (4)$$

For even  $d$  it maps the real line into a product of  $d/2$  unit circles, by winding it around each of the circles with stretch factor defined by the corresponding  $\theta_r$ . In Vaswani et al. (2017), the positional embeddings were defined as

$$p_{ij} = F_j^\theta(i) \quad (5)$$

with  $\theta_r$  being a geometric progression interpolating between 1 and some big number  $M$ .

To compute the winding embeddings, we first normalize the bounding boxes by scaling and translation. This causes the page bounding box to take the form  $(0, 0, w, h)$ , where  $w$  and  $h$  are the normalized width and height of the page, the larger of them equal to 1. Then, we use the function  $F^\theta$  to transform the coordinates of the normalized bounding boxes and finally concatenate the four resulting vectors. We use scaling factors  $(\theta_r)$  forming a geometric progression interpolating between 0.25 and 500.

### 3.3.2 Autoencoder embeddings

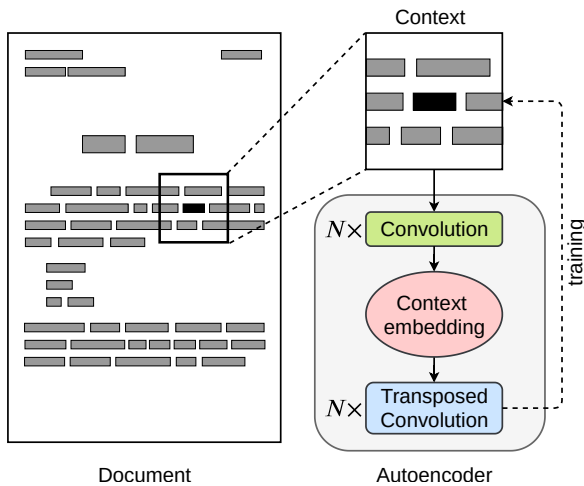


Figure 1: Autoencoder embeddings

*Autoencoder embeddings*<sup>1</sup> are defined using methods from image processing. First, the average line height  $h$  in the document is determined. Then, for each token, we consider its square neighborhood with side length  $Nh$ , where the optimal value for  $N$  was experimentally determined to be  $N = 22$  (corresponding to 350px in the initial experiments). The neighborhood is transformed into a  $64 \times 64$  black and white bitmap by placing black rectangles corresponding to token bounding boxes onto a white background. This image representation of the neighborhood is then encoded by an autoencoder, trained on a subset of the training set, yielding the context embedding of the token.

We use a convolutional autoencoder, whose encoder is a stack of convolutional layers with stride 2, each of them halving the dimensions and doubling the number of channels of its input. The decoder is built analogously from transposed convolutional layers. Since we fix the dimensions of the neighborhood representation to  $64 \times 64 \times 1$  (one binary channel), both the encoder and decoder contain  $\log_2 64 = 6$  layers. See Figure 1 for the diagram of this architecture.

### 3.3.3 Graph embeddings

Graph neural networks (GNNs) provide a framework to deal with data whose structure is described by a graph. More precisely, let  $G = (V, E)$  be a graph, and let  $f: V \rightarrow \mathbb{R}^d$  a function that assigns to each vertex  $v \in V$  its feature vector  $f(v) \in \mathbb{R}^d$ .

<sup>1</sup>Autoencoder embeddings were introduced in the (unpublished) MSc thesis of Bartosz Topolski

Generally speaking, a GNN computes vertex embeddings for the graph  $G$  endowed with vertex feature vectors described by  $f$ . In other words, it defines an operator from  $\mathbb{R}^d$ -valued functions on  $V$  to  $\mathbb{R}^t$ -valued functions on  $V$  for some output dimension  $t$ .

**Graph structure** Given a document with segmentation, we turn it into a graph whose vertices correspond to segments. To define the edges, we first independently normalize the vertical and horizontal coordinates, so that on average the bounding boxes of segments are square. Then, we choose a distance function (not necessarily a metric) and join each vertex to its  $K$  nearest neighbors (the upper left corners of bounding boxes were used for calculating distances).

As a distance we chose  $\ell^p$  with  $p = 1/2$ . It promotes neighbors in the same row or column as the original segment, over the diagonally positioned ones. We experimentally determined the optimal value  $K = 5$ .

**Architecture** Our context embeddings are based on the Graph Isomorphism Network (GIN) (Xu et al., 2018), whose main building block is the operator  $\mathcal{A}$  defined by

$$\mathcal{A}f(v) = (1 + \epsilon)f(v) + \sum_{w \sim v} f(w), \quad (6)$$

which for each vertex  $v$  of the graph aggregates the features of its neighbors by summing them, and combines them with the feature vector of  $v$ . In our setting, we assign  $\epsilon = 0$ .

In the original GIN architecture, a single block consists of the operator  $\mathcal{A}$  followed by a multi-layer perceptron, and this is also the case in our network. We use two linear layers with ReLU activations, followed by batch normalization. In Figure 2, the architectures of a *GIN block* and a *GIN module* consisting of three GIN blocks are presented. The network computing the context embeddings is a stack of 2 GIN modules followed by a linear layer. The input dimension of the network is 4 (the feature vector of a segment is simply its bounding box), the output dimension of the final linear layer is 128, and all the hidden dimensions (except the output dimensions of GIN modules) are set to 64.

## 4 Experiments

We based our evaluation on an end-to-end task, as this is the most meaningful information from the

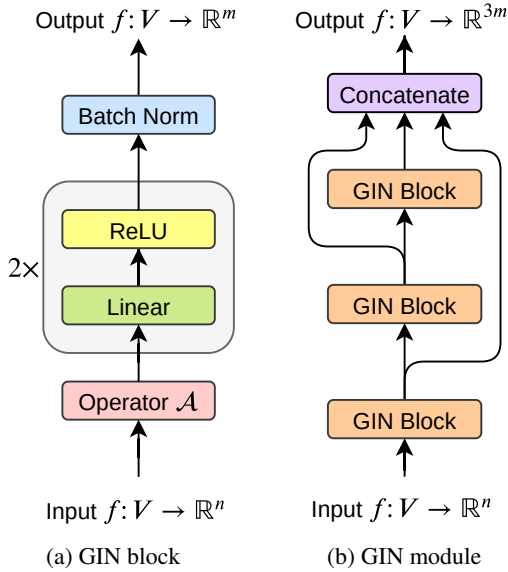


Figure 2: Architecture diagrams of a single GIN block and a GIN module.

practical point of view. Both BERT and RoBERTa were used in their smaller, base variants. Their implementations from the *pytorch-transformers* library by Hugging Face (2019) were used.

The models were trained on a language modeling task with layout information; and subsequently, on downstream information extraction tasks. In the remainder of the paper, these two stages will be referred to as *training* and *fine-tuning*, respectively.

## 4.1 Training

To train the models, we used a masked language modeling task, similar to the one used in the original BERT training.

### 4.1.1 Datasets

To train the models, we used a combination of 8 datasets (some of them publicly available and some private) containing a variety of documents with non-trivial layout:

Dataset	pages
EDGAR	119 088
RVL-CDIP	90 054
Common Crawl	389 469
cTDaR	782
private	151 074
<b>Total</b>	<b>750 467</b>

Table 1: Sizes of training datasets.

**EDGAR** This dataset was retrieved from the Electronic Data Gathering, Analysis and Retrieval (EDGAR) system (SEC, 2019), made publicly available by the U.S. Securities and Exchange Commission. It consists of forms (10-K, 20-F, and 40-F) submitted by companies supervised by SEC.

**RVL-CDIP** The Ryerson Vision Lab Complex Document Information Processing (RVL-CDIP) dataset (Harley et al., 2019) consists of 400k scanned pages of documents of various kinds, including letters, forms, invoices, advertisements, scientific reports, and many others.

**Common Crawl PDFs** This is a dataset produced by downloading PDF files pointed to by links in Common Crawl (2019). From each domain, only one file was randomly chosen and downloaded.

**cTDaR** The dataset from ICDAR 2019 Competition on Table Detection and Recognition (cTDaR) (ICDAR, 2015), containing various kinds of tables, both modern and historical. We used only modern ones.

**Private datasets** We also included four datasets containing private documents, mostly financial reports and filled forms.

### 4.1.2 Data preprocessing

The datasets underwent a procedure of removing undesirable documents. First, we discarded documents classified as handwritten and scanned documents with low OCR quality. Among the documents that could be reliably transformed into our data model, we filtered out all that could not be identified as written in English.

Based on the observation that pages containing plain text have more tokens than those with more interesting layouts, containing tables, we removed all pages with either more than 1000 or less than 50 tokens. Some more complex heuristics based on the distribution of the number of tokens in separate lines were also used to further avoid pages suspected of containing just a large block of text. The sizes of datasets after filtering are presented in Table 1.

All the documents were tokenized using the Byte Pair Encoding (BPE) tokenizer distributed together with the corresponding pretrained model, thus subdividing the original tokens. The bounding boxes were interpolated, under the assumption that all characters in a token have equal width.

Dataset		pages	attributes
Charity	train	36911	13458
	dev	10639	3436
	test	14672	4783
NDA	train	1486	1087
	dev	431	376
	test	747	765

Table 2: Kleister dataset sizes.

Since BERT imposes a limit on the number of tokens in the input sequence, we simply divided longer pages into chunks, according to the sequential order of tokens.

### 4.1.3 Setup

All experiments were performed on a single Tesla V100 GPU with 16 GB memory. We used the Adam optimizer with weight decay fix from [Hugging Face \(2019\)](#). We employed a learning rate scheduling method similar to the one used by [Devlin et al. \(2019\)](#), increasing the learning rate linearly for the warm-up period of 10% of the training time and then decreasing it linearly to 0.

The models were trained with batch size of 128 sequences (i.e. 65536 tokens) for approximately 150k steps, corresponding to 20 epochs over a 0.5 billion word corpus. For comparison, this is around 1/13 of training needed to pretrain the original 12-layer BERT model. Each training took approximately 5 days to complete.

## 4.2 Fine-tuning

After training our models, we fine-tuned them on downstream information extraction tasks, in order to evaluate their performance in an end-to-end setting.

### 4.2.1 Datasets

For fine-tuning and evaluation on downstream tasks, we used the *Kleister* datasets.<sup>2</sup> These datasets are a new collection of datasets created in order to evaluate end-to-end solutions for extracting information from complex documents. They contain noisy multi-modal input, forms, tables, etc. Their sizes are presented in Table 2.

<sup>2</sup>They are to become publicly available in the near future; their authors allowed us to use them earlier for the purpose of this paper. We included some examples of documents from these datasets in the supplementary material.

Note that information extraction is more difficult than entity recognition. In the latter case, the desired information occurs directly in the text, while in the former, retrieving the information may require normalization, and in more complex scenarios, synthesis of the clues dispersed in the document. The Kleister datasets merely provide the correct values of extractable attributes (or the information that the attribute does not appear in the document), without specifying their source in the document text.

**Kleister-Charity** This dataset is composed of financial reports of charities registered in England and Wales, made publicly available by the Charity Commission for England and Wales. There is no fixed format of such a report, and the documents in the dataset are diverse. Some have only a few pages filled with the key information, while others are long, richly illustrated, and full of tables and charts.

The eight extractable attributes in the documents include separate address components (street line, post code, post town); charity names; identification numbers; report date; and annual income and spending amounts.

**Kleister-NDA** The dataset is composed of non-disclosure agreements found in attachments to other contracts or forms in the EDGAR database (see Section 4.1.1). Their layout is quite regular, and being legal agreements, they have hierarchical structure with many sections and subsections.

Each document contains six attributes to be extracted, such as the duration of the contract, or the date after which it becomes legally binding.

### 4.2.2 Data preprocessing

We chose to approach the problem of information extraction through entity recognition, by tagging entity types of tokens. This method requires a suitably tagged training dataset, hence we had to perform automatic tagging of documents in the Kleister datasets. Consequently, the quality of this *auto-tagging* procedure impacts the overall end-to-end results. A more detailed discussion of the autotagging procedure is outside the scope of this paper.

### 4.2.3 Setup

The model was extended with a simple classification head on top, consisting of a single linear layer, and fine-tuned on the task of classifying entity types of tokens. Fine-tuning on each of the

Model			$F_1$ -score			
name	context embeddings	trained on our data	NDA	Charity		
				income	spending	all
BERT	—	○	0.700	0.456	0.452	0.695
	—	●	0.745	0.522	0.491	0.710
LAMBERT (on BERT)	winding	●	0.716	0.608	0.584	0.744
	autoencoder	●	0.726	0.565	0.544	0.724
	graph	●	0.732	0.540	0.505	0.730
RoBERTa	—	○	0.725	0.478	0.500	0.716
	—	●	0.745	0.546	0.575	0.748
LAMBERT (on RoBERTa)	winding	●	0.739	0.599	0.588	0.756
	winding-only*	●	0.741	<b>0.667</b>	<b>0.638</b>	<b>0.775</b>
	autoencoder	●	0.747	0.591	0.559	0.760
	graph	●	0.751	0.592	0.560	0.759

Table 3: End-to-end evaluation results on Kleister datasets. \**Winding-only* stands for winding embeddings with suppressed sequential information, as described in Section 4.3.

Kleister datasets was performed separately.

We used the same hardware configuration as for model training (Section 4.1.3). The models were trained with early stopping, based on the  $F_1$ -score achieved on the development set. We used the Adam optimizer, but this time without the learning rate warm-up, as it turned out to have no impact on the results.

### 4.3 Suppressing sequential order

As a part of our final experiment, we attempted to suppress the sequential information in the RoBERTa-based model using the winding embeddings, in order to study its ability to completely switch from using positional embeddings to layout embeddings. We modified the input embeddings from eq. (2) by composing the positional embedding term  $p_i$  with unnormalized dropout with probability  $q$ .

For the first half of training, the parameter  $q$  was linearly increased from 0 to 1, and it remained equal to 1 afterwards; thus effectively disabling the positional embeddings  $p_i$  and leaving the model only with the layout embeddings  $\ell_i$ .

### 4.4 Evaluation

The extended model outputs a classification of tokens, while the datasets contain only the values of extractable attributes. Therefore, further processing of output is required. Every contiguous sequence of tokens tagged as a given entity type is

treated as a recognized entity and assigned a score equal to the geometric mean of the scores of its constituent tokens.

Then, every recognized entity undergoes a normalization procedure specific to its general data type (e.g. date, monetary amount, address, etc.), and duplicates are aggregated by summing their scores, giving bias to entities detected multiple times. Finally, the highest-scoring normalized entity is selected as the output of the information extraction system.

The predictions obtained this way are compared with target values provided in the dataset using  $F_1$ -score as the evaluation metric.

### 4.5 Results

In Table 3, we present the evaluation results achieved on downstream tasks by the best models based on pretrained BERT and RoBERTa, using the context embeddings described in Section 3.3.

For comparison, we also included evaluation of two variants of original pretrained models (i.e. without context embeddings), the first one both trained and fine-tuned, and the second only fine-tuned.

In the Charity dataset, we singled out the results for extraction of income and spending amounts. These attributes usually appear in large tables containing many other numerical values. Moreover, for such tables, the reading order produced by the OCR is often column by column, so the proper alignment of tokens into rows must be deduced

by the model from the layout information. This is the kind of problem where adding the layout embeddings should significantly improve the results. This is indeed the case seen when using the winding embeddings, especially the one with disabled positional embeddings.

To further investigate this claim, we prepared some visualizations of the attention weights. In Figure 3a, we present a document with tabular data laid out in two columns. The OCR recognized the document as a two-column text, i.e. it produced a reading order in which all the tokens in the left column precede the tokens in the right column. Relying only on this order is not enough to tie the keys in the left column with corresponding values on the right.

We used our layout-only model to compute the embeddings of tokens in this document, and visualized its attention weights. We have found that some heads rely on relative positions of tokens. An example is pictured in Figure 3, where we can see that the head correctly ties the values in the right column with the corresponding row labels. More visualizations are included in the supplementary material.

## 5 Conclusions

The first conclusion is that providing the layout information improves the model performance on tasks where graphical features are useful, while it does not lead to deterioration when dealing with flat layout. Not only this, but after completely replacing the sequential position signal with the layout embeddings in the rich-layout Charity dataset, the results improve even more.

It means that whatever can be inferred from the sequential order of tokens, the model is able to deduce from their positions on the page, and the original positional embeddings seem to be only a distraction when they are accompanied by the layout embeddings.

This has an intuitive explanation—in eq. (2) we are summing three terms containing different pieces of information, which has to be subsequently extracted by the model. The more summands are used, the more difficult it is to learn how to retrieve the information they carry. If one of the terms is redundant, it imposes the cost of an additional summand without giving any new benefits in return.

We also see that the winding embeddings achieve similar or better performance than their

Date of incorporation	4 April 2006
Company registration number	5769138
Charity registration number	1117506
Registered office	30 Finsbury Circus London EC2M 7DT
Board of Directors	C N Billingham A J Cowan D McCarthy
Company secretary	P M Rogers
Bankers	Barclays Bank plc. 8/9 Hanover Square London W1A 4ZW

(a) Original document

Date of incorporation	4 April 2006
Company registration number	5769138
Charity registration number	1117506

(b) Attention for a token in the first row

Date of incorporation	4 April 2006
Company registration number	5769138
Charity registration number	1117506

(c) Attention for a token in the second row

Date of incorporation	4 April 2006
Company registration number	5769138
Charity registration number	1117506

(d) Attention for a token in the third row

Figure 3: Visualizations of one of the attention heads. The word for which the embedding is computed is marked with a contour and attended words are highlighted.

much more complicated counterparts; in our case the simpler turned out to be the better. The Transformer has the capacity to utilize the information contained in plain bounding box coordinates, and altering this information only hinders this ability. It might be well possible to come up with context embeddings materially outperforming the winding embeddings, but it looks like a non-trivial task.

Also, models based on RoBERTa surpass those based on BERT, which is not surprising. It shows that the representations learned during pretraining are preserved through our procedure, which only extends them with layout information.

Finally, note that while using the winding embeddings in the Charity dataset improves the results of the plain models, in the NDA dataset they remain similar for RoBERTa and worsen in case of BERT. The RoBERTa behavior again confirms that the model can effectively utilize the layout features,



without forsaking what it learned during pretraining. In case of BERT, this could be caused by the small size of the NDA dataset.

## References

- Amazon. 2019. Amazon textract. <https://aws.amazon.com/textract/> (accessed November 25, 2019).
- Common Crawl. 2019. Common Crawl. <https://commoncrawl.org> (accessed December 6, 2019).
- Zihang Dai, Zhilin Yang, Yiming Yang, Jaime Carbonell, Quoc Le, and Ruslan Salakhutdinov. 2019. Transformer-XL: Attentive language models beyond a fixed-length context. In *Proceedings of the 57th Annual Meeting of the Association for Computational Linguistics*, pages 2978–2988, Florence, Italy. Association for Computational Linguistics.
- Timo I. Denk and Christian Reisswig. 2019. **BERT-grid: Contextualized embedding for 2D document representation and understanding**.
- Jacob Devlin, Ming-Wei Chang, Kenton Lee, and Kristina Toutanova. 2019. **BERT: Pre-training of deep bidirectional transformers for language understanding**. In *Proceedings of the 2019 Conference of the North American Chapter of the Association for Computational Linguistics: Human Language Technologies, Volume 1 (Long and Short Papers)*, pages 4171–4186, Minneapolis, Minnesota. Association for Computational Linguistics.
- Google. 2019. Cloud Document Understanding AI. <https://cloud.google.com/document-understanding/docs/> (accessed November 25, 2019).
- Adam W Harley, Alex Ufkes, and Konstantinos G Derpanis. 2019. Evaluation of deep convolutional nets for document image classification and retrieval. In *International Conference on Document Analysis and Recognition (ICDAR)*. <http://www.cs.cmu.edu/~aharley/rvl-cdip/> (accessed November 26, 2019).
- Hugging Face. 2019. Transformers. <https://github.com/huggingface/transformers> (accessed November 27, 2019).
- ICDAR. 2015. Competition on Table Detection and Recognition. <http://sac.founderit.com/index.html> (accessed November 26, 2019).
- Anoop R Katti, Christian Reisswig, Cordula Guder, Sebastian Brarda, Steffen Bickel, Johannes Höhne, and Jean Baptiste Faddoul. 2018. **Chargrid: Towards understanding 2D documents**. *Proceedings of the 2018 Conference on Empirical Methods in Natural Language Processing*.
- Zhenzhong Lan, Mingda Chen, Sebastian Goodman, Kevin Gimpel, Piyush Sharma, and Radu Soricut. 2019. **ALBERT: A lite BERT for self-supervised learning of language representations**.
- Xiaojing Liu, Feiyu Gao, Qiong Zhang, and Huasha Zhao. 2019a. **Graph convolution for multimodal information extraction from visually rich documents**. *Proceedings of the 2019 Conference of the North*.
- Yinhan Liu, Myle Ott, Naman Goyal, Jingfei Du, Mandar Joshi, Danqi Chen, Omer Levy, Mike Lewis, Luke Zettlemoyer, and Veselin Stoyanov. 2019b. **RoBERTa: A robustly optimized BERT pretraining approach**.
- Microsoft. 2019. Cognitive Services. <https://azure.microsoft.com/en-us/services/cognitive-services/> (accessed November 25, 2019).
- Alec Radford. 2018. Improving Language Understanding by Generative Pre-Training.
- Alec Radford, Jeff Wu, Rewon Child, David Luan, Dario Amodei, and Ilya Sutskever. 2019. Language models are unsupervised multitask learners.
- Wasifur Rahman, Md Kamrul Hasan, Amir Zadeh, Louis-Philippe Morency, and Mohammed Ehsan Hoque. 2019. **M-BERT: Injecting multimodal information in the BERT structure**.
- SEC. 2019. Electronic Data Gathering, Analysis and Retrieval system. <https://www.sec.gov/edgar.shtml> (accessed November 26, 2019).
- Yusuke Shinyama. 2019. PDFMiner. <https://github.com/euske/pdfminer> (accessed November 25, 2019).
- Ashish Vaswani, Noam Shazeer, Niki Parmar, Jakob Uszkoreit, Llion Jones, Aidan N Gomez, Łukasz Kaiser, and Illia Polosukhin. 2017. **Attention is all you need**. In I. Guyon, U. V. Luxburg, S. Bengio, H. Wallach, R. Fergus, S. Vishwanathan, and R. Garnett, editors, *Advances in Neural Information Processing Systems 30*, pages 5998–6008. Curran Associates, Inc.
- Alex Wang, Amanpreet Singh, Julian Michael, Felix Hill, Omer Levy, and Samuel R. Bowman. 2019. GLUE: A multi-task benchmark and analysis platform for natural language understanding. In *Proceedings of ICLR*. <https://gluebenchmark.com/> (accessed November 26, 2019).
- Keyulu Xu, Weihua Hu, Jure Leskovec, and Stefanie Jegelka. 2018. **How powerful are graph neural networks?**
- Zhilin Yang, Zihang Dai, Yiming Yang, Jaime Carbonell, Ruslan Salakhutdinov, and Quoc V. Le. 2019. **XLNet: Generalized autoregressive pretraining for language understanding**.